Survey of WO₃ thin film structure built on ITO/glass substrates by the Raman and XRD spectroscopies

Le Van Ngoc[1,*], Tran Cao Vinh[1], Le Quang Toai[1], Nguyen Duc Thinh[1]
Huynh Thanh Dat[2], Tran Tuan[1], Duong Ai Phuong[1]

[1] *University of Science, Vietnam National University - Ho Chi Minh city, 227 Nguyen Van Cu, Vietnam*
[2] *Vietnam National University - Ho Chi Minh city, Linh Trung, Thu Duc, Vietnam*

Abstract. Tungsten oxide film was deposited on ITO-coated glass by using RF magnetron sputtering method from WO₃ ceramic target. Thin film preparation – process took place in Ar + O₂ plasma. The dependence of tungsten oxide film structure on experiment conditions was investigated by X-ray diffraction (XRD) Raman spectroscopy. In this paper, we considered that the thickness of ITO layers about 150 nm to 350 nm clearly effects on the Raman and XRD spectrograms of WO₃ films.

Keywords: WO3 structure, WO3 /ITO/glass, Raman spectroscopy.

1. Introduction

WO₃ thin films have been studied for a long time due to their unique properties and potential applications. And the most promising application of WO₃ thin films is electrochromic devices based on electrochromism, in which optical properties WO₃ alter reversibly under electrical bias applied [1-3]. Moreover, recently WO₃ thin films have been studied to fabricate toxic gas sensors, such as NO_x, H_2S, NH_3, CO and some popular others like H_2, O_2, O_3, Cl_2, SO_2, CH_4 [4-7]. Both electrochromism and gaseous sensitization are based on the reversible diffusion of particles along the vacant tunnels of WO₃ perovskite structure. Thus, having large and oriented vacant tunnels will be a great advantage.

Furthermore, many methods are used to prepare WO₃ thin films, such as sputtering [8-11], sol – gel [12], spray pyrolysis [13-14], anodizing technique [15], thermal evaporation [15-21]. And different preparation methods have respective advantages in film quality and application.

Besides optical and electrical properties, WO₃ crystalline structure has been studied by utilizing XRD and Raman Spectroscopy. XRD surveys focus on 20° – 25° range of diffraction angles and Raman spectroscopy surveys focus on 200 cm⁻¹ – 1000 cm⁻¹ range of wave number.

In this paper, WO₃ layers were deposited on ITO/glass substrates. The thickness of ITO layers is measured approximately 150, 200, 250, 300, 350 nm, respectively. From XRD spectrograms, we considered that the thickness of ITO coaters clearly effect on WO₃ crystalline structure. In order to

---

* Corresponding author. Tel.: 0908283530
E-mail: lvngoc@phys.hcmuns.edu.vn

understand what occurred inside and whether nano particle phases exist, we used their Raman spectroscopy. And 600 cm^{-1} – 1000 cm^{-1} range was analyzed into different basic vibration. With samples with ITO layer about 300nm thickness and more, in Raman spectrum there is an odd peak at 680 cm^{-1}, which could be related to nano phases. However, the absence of 950 cm^{-1} refuses that assumption. The origin of this peak will be focused on in this paper.

2. Experimental

In this research, ITO and WO_3 layers were prepared by magnetron sputtering in (O_2 + Ar) plasma. Oxygen and argon gases with high purity (99.999%) were used in deposition processes. Our sputtering chamber was evacuated down to 10^{-7} torr by using turbo pump before introducing gases. ITO layers were deposited on glass substrates by DC magnetron sputtering with their thickness about 150, 200, 250, 300, 350 nm respectively. Then WO_3 layers were deposited on ITO/glass by RF magnetron sputtering. The power is 100 W and the deposition time is about 30 minutes.

After deposition, WO_3/ITO/glass systems were annealed in the atmosphere at 400°C temperature during four hours. The crystalline structure of WO_3 thin films was investigated by XRD patterns using Cu K_α radiation at 1.5406 Å wavelength and Raman spectroscopy using He – Ne excitation (632.8 nm). In order to analyze broad peaks, included many basic vibration modes of Raman spectrum, we used Origin 7.5 program with Gaussian function. This information gives us exact evaluation of the existence of different phases in our films.

3. Results and discussion

3.1. The effect of the thickness of ITO layer on XRD spectrum

All WO_3 thin films, created in these experimental conditions, were transparent in visible region. In order to study their structural properties, we used XRD spectrum with an attention to 22° – 25° range of 20 diffraction angle due to the existence of three highest peaks. Figure 1 shows XRD pattern of WO_3 powder sample with three peaks with strongest magnitudes (001), (020), (200). They correspond with 20 = 23.29°, 23.77°, 24.51° with lattice plane distances d = 0.382 nm, 0.374 nm, 0.363 nm, respectively. Therefore, our WO_3 powder sample has a monoclinic structure (m-WO_3) with α = γ =90°, β = 90.15°, a = 0.7285 nm, b = 0.7517 nm, c = 0.3835 nm [22] and two highest peaks, located at (001) and (200) (international JCPDC database, JCPDC 5 - 363).
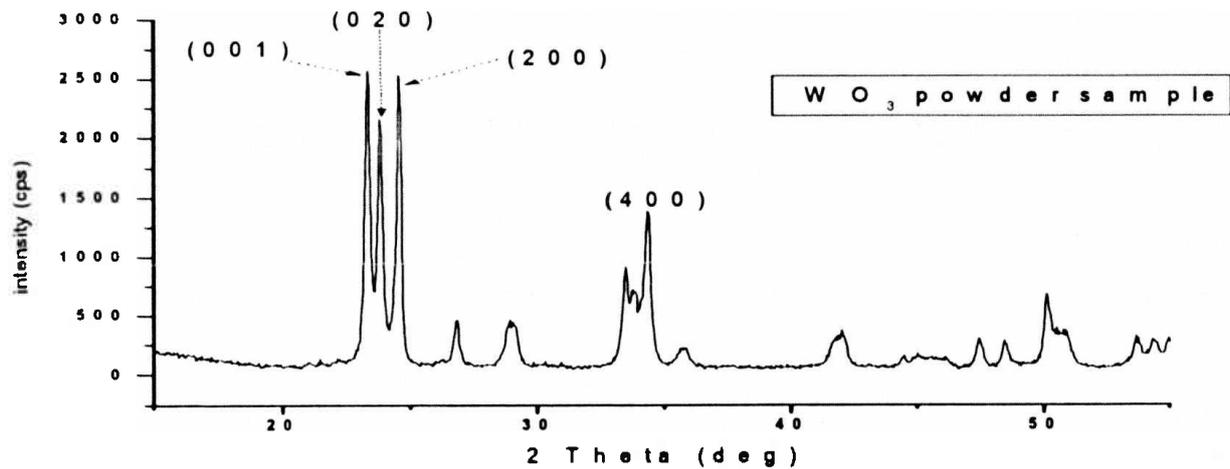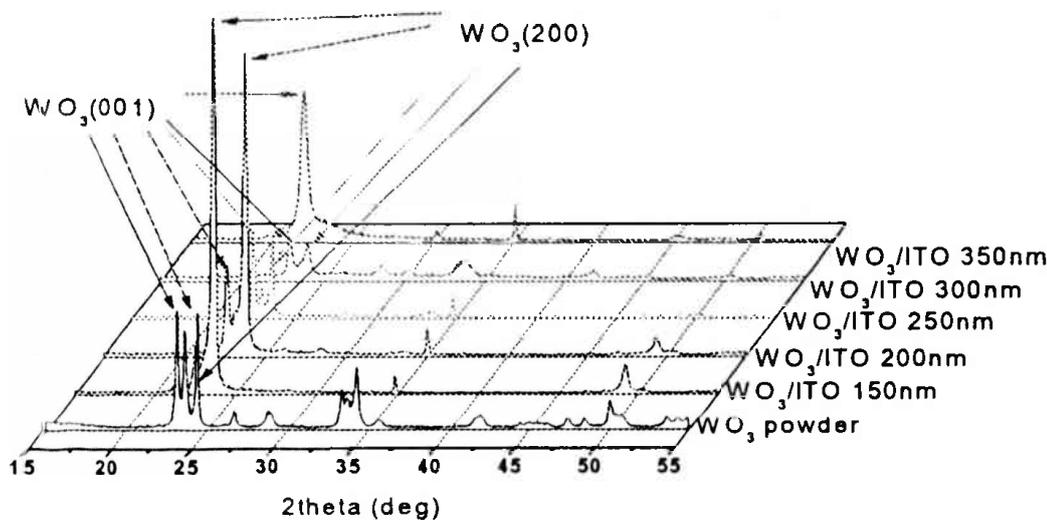
Fig. 1. XRD spectrum of m-WO₃ powder.

Fig. 2. XRD spectra of WO₃ films on layers ITO with different thicknesses.

Figure 2 is XRD spectra of films on layers ITO with different thicknesses. However their peaks distribute in such a small range of the angle 2θ, that we couldn't confirm whether our films have a monoclinic structure (with parameters $\alpha = \gamma = 90^0$, $\beta = 90,15^0$, and a = 0,7285 nm, b = 0,7517 nm, c = 0,3835 nm) or a orthorhombic one (o-WO₃ with $\alpha = \beta = \gamma = 90^0$, a = 0,7341 nm, b = 0,7570 nm, c = 0,3877 nm) because the values aren't clearly distinctive.

Analyzing figure 2, we recognized that ITO layer with thickness about 150 nm, XRD shows a sharp peak (200), accompanied by a weaker one (001). Between these peaks was a even weaker peak (020), like a shoulder of (200) font. With an increase in the thickness from 150 nm to 350 nm, XRD spectra expose a gradual decrease of the magnitude of peak (200) and a raise of peak (001). Moreover, peak (020) is shown obviously in the case of 250 nm. When the ITO layer have a thickness about 300 nm, a growth of WO₃ show a great anomaly in orientation due to the appearance of peaks in larger diffraction angles. With 350 nm thickness ITO player, WO₃ film preferentially grows along direction (001) with larger lattice plane distance (0.4001 nm). This value is nearly equal to (001) lattice plane

distance of tetragonal structure (t-WO_3). Therefore, we assumed that the crystalline structure of this WO_3 film is tetragonal (with $\alpha = \beta = \gamma = 90°$, a = b = 0.525 nm, c = 0.392 nm). With this structure, vacant tunnels along c – axis are narrower than these ones of m-WO_3 and o-WO_3. WO_3 film preferentially grow along direction (001), (200), however, both of these two possible growth directions lead us to the conclusion that vacant tunnels grew perpendicular to film surface. And with preferentially growing along (200) direction of o-WO_3, vacant tunnels achieved the largest size of WO_3 – perovskite.

In this research, all the peaks of WO_3 film in XRD spectra are shifted to smaller diffraction angles than these ones of powder sample. This result shows that the lattice plane distance increases due to a compressed stress, because WO_3 has a coefficient thermal expansion smaller than glass does and because of the heteroepitaxial growth of films WO_3 in which the parameters of plane ITO (440) are slightly larger than the ones of WO_3 planes. The relation between shifts of XRD peaks and total film stress is given by equation:

$$\sigma_f = \frac{E}{4\upsilon} \frac{\Delta(2\theta)}{\tan\theta}$$

Where σ_f is total film stress, θ is Bragg diffraction angle, E is Young modulus, υ is Poisson coefficient. $\Delta(2\theta)$ will get a minus value if the total film stress is compressed stress [23]. Thus due to this thermal stress, in order to survey WO_3, we have combined the results from both XRD and Raman spectrum investigations. Beside that, from XRD patter, the grain size of WO_3 film were determined by Scherrer equation and all of them valued in 30 nm to 35 nm.

3.2. Micro – Raman Studies

Due to structural modifications of WO_3 films, deposited on of ITO layers with different thicknesses, we investigated their Raman spectra to find out more helpful information. We divided ITO layers into two groups, basing on their thicknesses: 150 – 250 nm group and 300 – 350 nm group.

3.2.1. Raman spectrum of WO_3 thin films on ITO layers with thickness, altering from 150 to 250 nm

Figure 3 shows XRD and Raman spectra of WO_3 powder sample and WO_3 films, deposited on ITO layers/150 nm, 200 nm and 250 nm thickness. Generally, these films have ratios $I_{(200)}/I_{(001)}$ in XRD pattern quite greater than this one of powder sample. Raman spectra of all three samples show sharp peaks, sited at 265.6 – 269.7 cm^{-1}, 703.8 – 709.9 cm^{-1} and 799.99 – 803.5 cm^{-1}. All these peaks are characterized for crystalline phase of WO_3. The Raman peak at 256.6 cm^{-1} indicates the deformation vibration of O – W – O bond and 600 – 900 cm^{-1} region relates to stretching vibrations of W – O bonds [24]. The Raman peak at 950 cm^{-1}, attributed to W = O boundary bonds does not exist. So we assumed that the surface and volume rate is negligible.

In the other hand, three sharp peaks, characterizing WO_3 crystalline phase, located at 263 cm^{-1}, 709 cm^{-1}, 802 cm^{-1} do not indicate any difference in structure between WO_3 films and WO_3 powder sample and between one film to another. These numbers show no difference in structure between WO_3 powder and WO_3 films. However, we could not eliminate a probability of orthorhombic phase in these films because the parameters of orthorhombic and monoclinic primary cells are nearly the same.

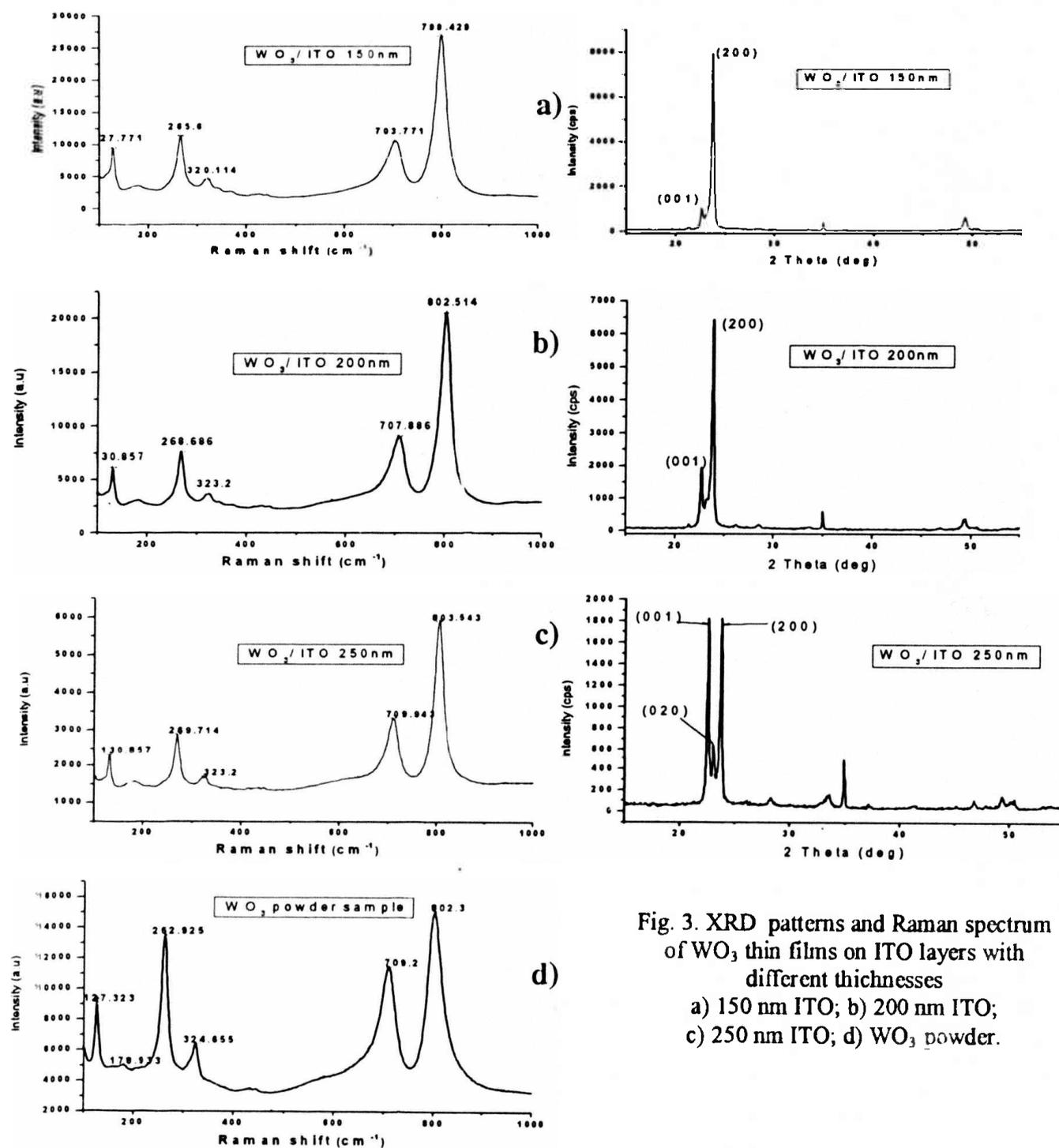### 3.2.2. Raman spectrum of WO₃ thin films on ITO layers with thickness, altering from 300 to 350 nm

Fig. 3. XRD patterns and Raman spectrum
of WO₃ thin films on ITO layers with
different thichnesses
a) 150 nm ITO; b) 200 nm ITO;
c) 250 nm ITO; d) WO₃ powder.

Figure 4 shows the Raman and XRD spectrum of WO₃ films, deposited on 300 nm and 350 nm ITO layers and WO₃ powder sample. From XRD spectra of WO₃ / ITO 300 nm film intensity of peak (001) exceeds intensity of peak (200). And WO₃ film, deposited on 350 nm ITO layer preferentially grew in (001) direction.
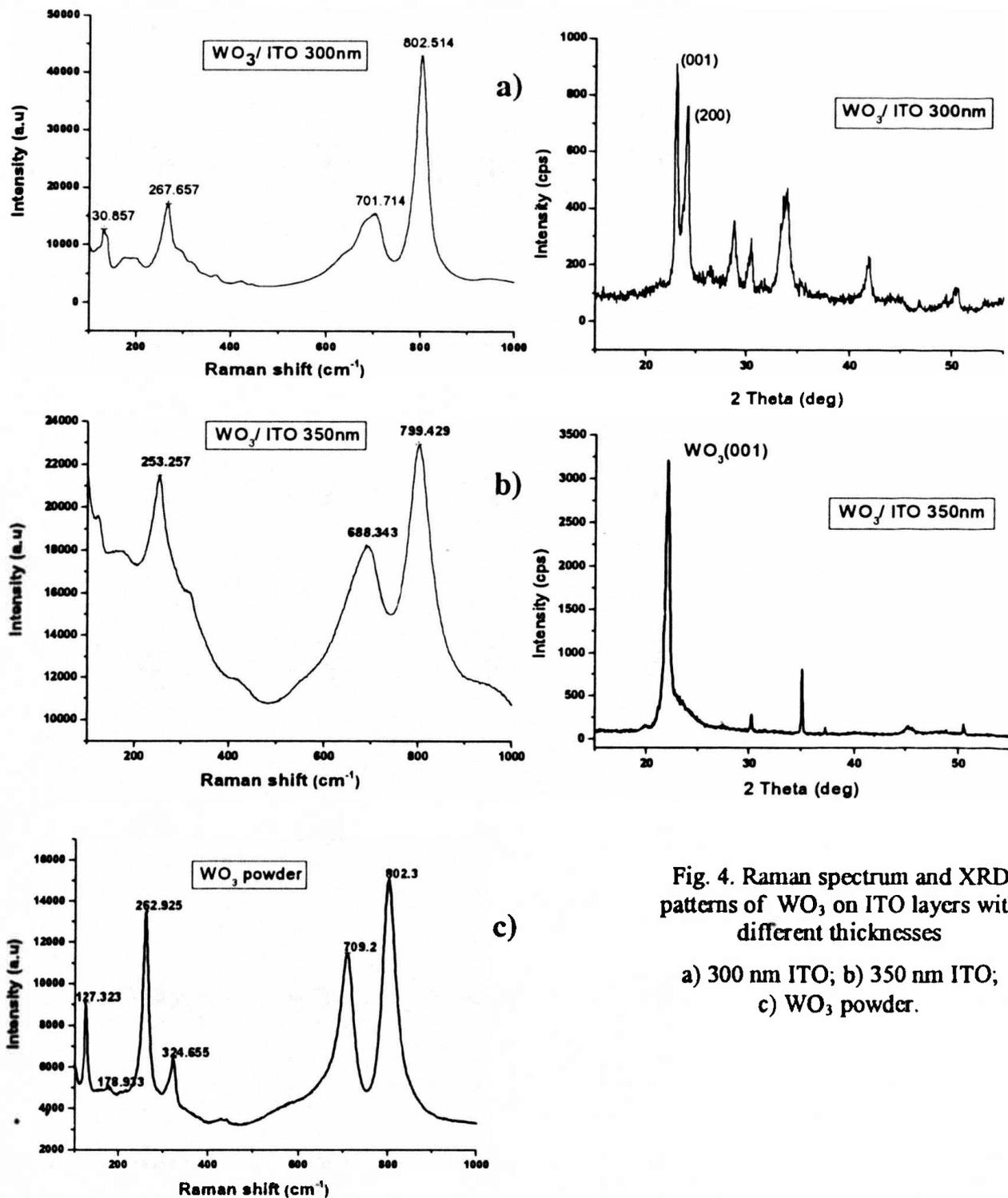
Fig. 4. Raman spectrum and XRD patterns of WO₃ on ITO layers with different thicknesses

a) 300 nm ITO; b) 350 nm ITO; c) WO₃ powder.

Comparing between XRD spectra of WO₃ films and WO₃ powder, we can not deduce any difference in crystalline structure. However, in the Raman spectrum of WO₃ /ITO 300 nm (fig. 4a) besides two characteristic peaks of crystalline structure, which are located at 267.66 cm^{-1} of the deformation mode and 802.5 cm^{-1} of covalent bonds W – O, there is only one clear modification, comparing to Raman spectra of film on thinner ITO layers. The only difference is a composition of two peaks, one at 680 cm^{-1} and the other at 709 cm^{-1}. And one possible reason is the existence of nano phases. [25]

Nevertheless, like Raman spectra of WO_3/ITO 150 nm, WO_3/ITO – 200 nm and WO_3/ITO – 250 nm, 950 cm^{-1} peak, which corresponds to W = O boundary bonds, does not appear due to the annealing process. It means that the ratio of surface to volume is negligible. And some calculations, basing on formula Scherrer also shows that the size of grains in all WO_3 films is about 30 – 35 nm. Moreover the annealing process and the breakage of the double bonds W = O also result in the limit of the shift to the 680 cm^{-1}. Thus, in the films WO_3/ITO 300 nm nanocrystal phase does not produce any strong peak about 680 cm^{-1}. Therefore, we believe that the appearance of peak closed to 680 cm^{-1} have another origin, such as phase tetragonal (t-WO_3) or phase orthorhombic (o-WO_3).

In order to understand more about the mentioned peak, we used program Origin 7.5 to analyze the doublet 701.7 cm^{-1} of thin film WO_3/ITO 300nm and investigated XRD and Raman spectra of WO_3/ITO 350 nm. Analyzing the spectra of WO_3/ITO 300 nm, we received one peak which is not sharp and corresponds to the vibration mode of WO_3-H_2O. The two other sit at 703 cm^{-1} and 678 cm^{-1}. And the best fit was get by considering the peak 802 cm^{-1} as a combination of two separated ones at 803 cm^{-1} and 797 cm^{-1} as shown in figure 5. Moreover, in some previous researches of other authors, there were only two peaks in the range from 600 to 900 cm^{-1}, which are attributed to covalent vibration of chemical bonds W – O in the octahedral WO_6 around W centers of lattice. Therefore, the existence of both four peaks 803 cm^{-1}; 797 cm^{-1}; 703 cm^{-1} and 678 cm^{-1} proves that in our thin films, there are two types of crystalline structures: m-WO_3 phase with 803 cm^{-1} and 703cm^{-1} and t-WO_3 phase or o-WO_3 phase with the two characteristic peaks at 797 cm^{-1} and 678 cm^{-1}.
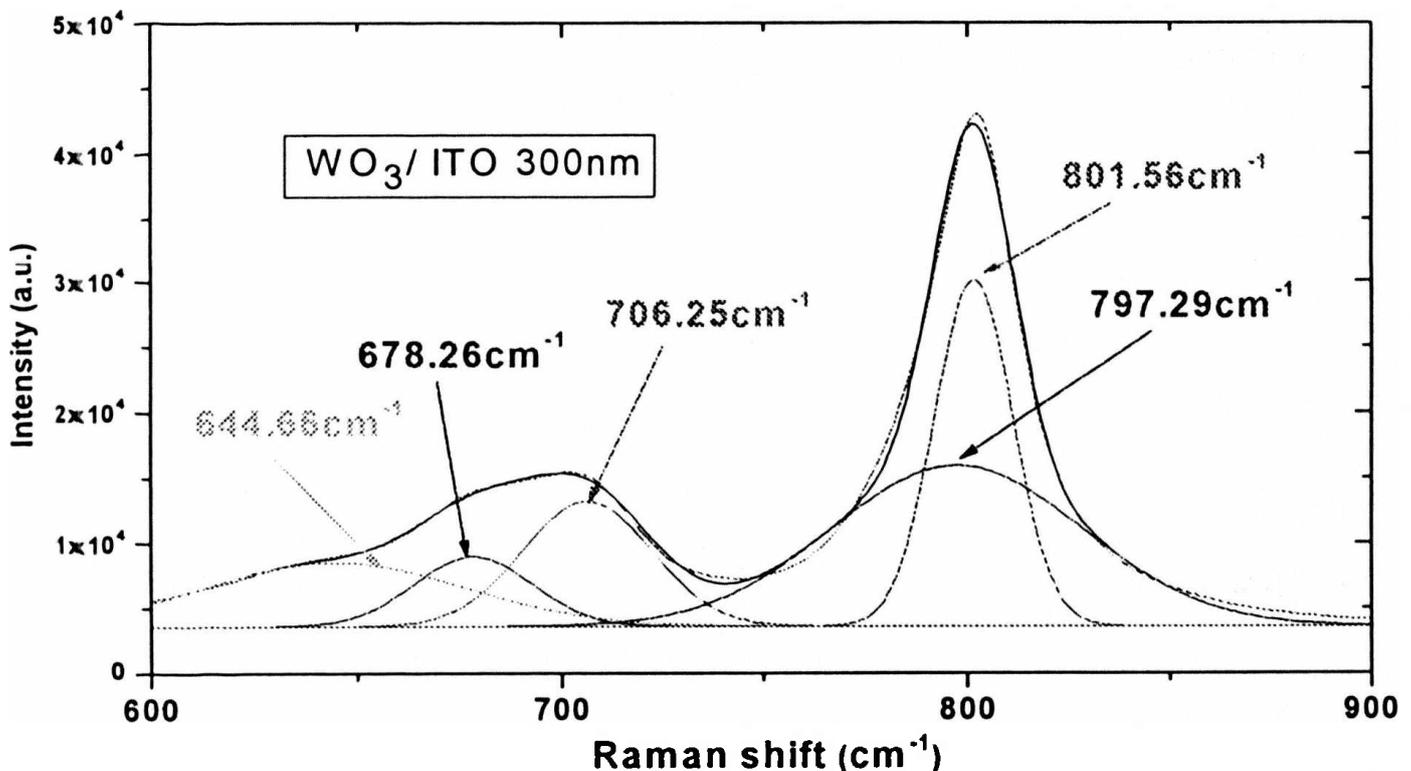

Fig. 5. Raman spectra of WO_3 thin film/ITO 300 nm/glass substrate.

However, from the experiments of E.Cazzanelli [26], the phase transition from orthorhombic phase to tetragonal phase is accompanied by the disappearance of peak at 700 cm^{-1}, only peak at 800 cm^{-1} remains. So, in WO_3/ITO 350 nm the t-WO_3 phase could not exist, the two possible ones are m-

WO_3 and o-WO_3. Therefore, we believed that a pair of peaks at 803 cm^{-1}; 708 cm^{-1} correspond to mo-WO_3 phases and the another pair goes for the o-WO_3 phases. In that case, the vibrational frequencies of m-WO_3 are quite higher than these of o-WO_3. And the reason is that parameters of crystalline structure of m-WO_3 are smaller than that of o-WO_3 or the force constant in W-O bonds in the former is larger than in the later phase.
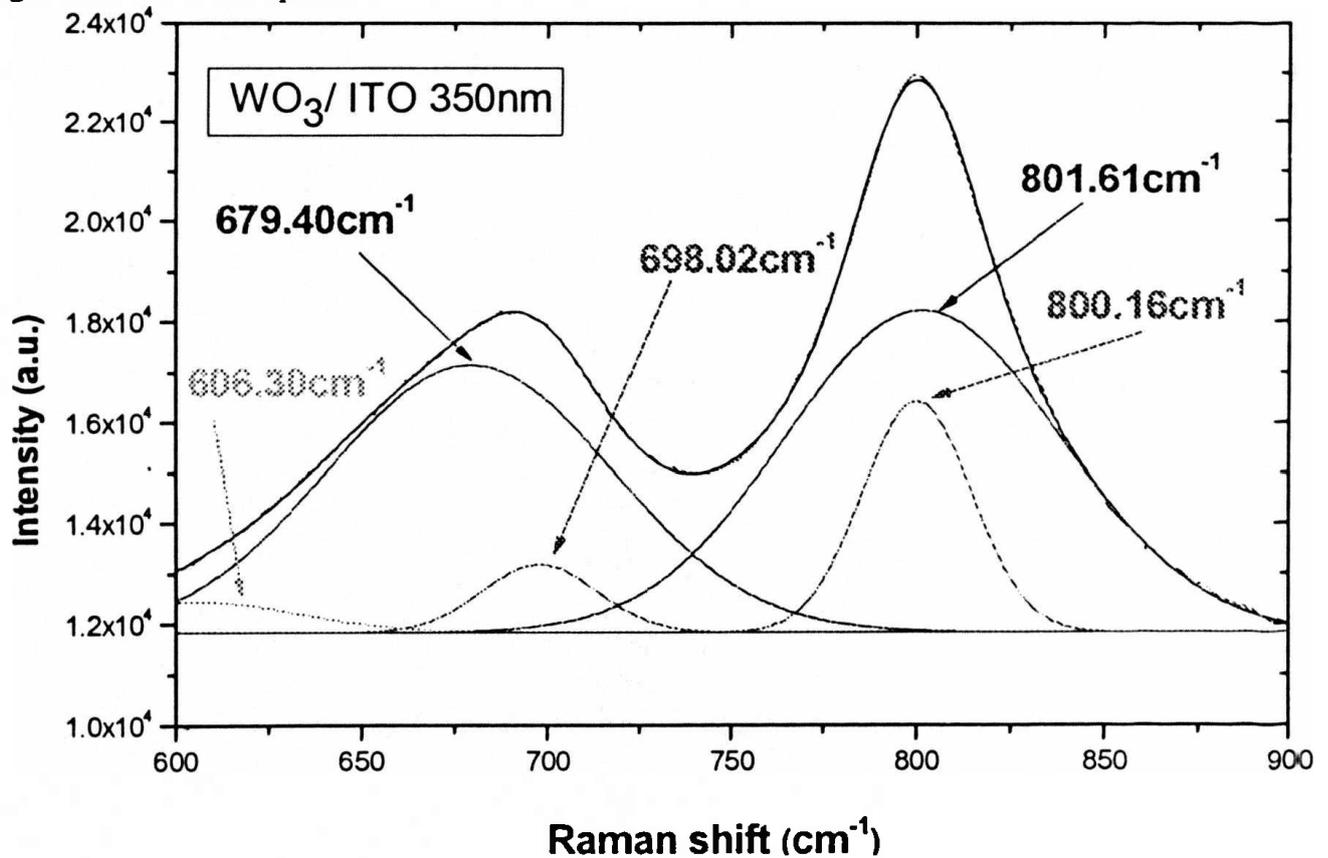

Fig. 6. Raman spectra of WO_3 thin film/ITO 350 nm/glass substrate.

XRD spectrum of WO_3/ITO 350 nm sample shows that WO_3 film grows along (001) direction preferentially, (020) and (200) peaks are weakened down to the font of (001) peak. In these films WO_3 particles are well crystallized. For a Raman spectrum of that film, peaks, characterizing crystalline phases, such as 799.4 cm^{-1}, 688.3 cm^{-1} and 253.26 cm^{-1} have appeared and the last two of them are shifted to smaller wave numbers, comparing to spectra 3a, 3b and 3c. Furthermore, peak 688,3 cm^{-1} in the spectrum of WO_3/ITO 350 nm is a combination of peaks at 680 cm^{-1} of o-WO_3 and at 700 cm^{-1} of m-WO_3 , where the former is much stronger than the later as shown in figure 6.

4. Conclusion

In this research, we have prepared WO_3 films on ITO/ glass substrates by magnetron sputtering and annealing in the atmosphere. With thin ITO coaters, 150 nm, WO_3 film grew along (200) plane preferentially. An increase in the thickness of ITO layer, WO_3 film orientation changes from (200) to (001) gradually.

In our experiments, films have many different crystalline structures with m-WO$_3$ and o-WO$_3$ to be the majority. With layer ITO with thickness 250 nm or thinner, the majority is m-WO$_3$ with Raman peaks at 263 cm^{-1}; 709 cm^{-1}; 802 cm^{-1}. However when the thickness is 300 nm or higher, the peaks, characterizing to orthorhombic phase at 797 cm^{-1}; 678 cm^{-1} emerge clearly. Films with thickness 300 nm could be regarded as a transitional phase with both m-WO$_3$ and o-WO$_3$ phases.

References

[1] C. G Granqvist, E.Alvendamo, A.Zeus, *Thin Solid Film* 442 (2003) 201.

[2] Vu Thi Bich, Nguyen Thanh Binh, Nguyen Thi Bich Ngoc, A.Hugot-Le Goff. Proc. IWOS'2000, Hanoi, Vietnam, 477.

[3] Pham Duy Long, M.C. Bernard, Nguyen Thi Tu Oanh, A.Hugot-Le Goff, Nguyen Nang Dinh. Proc. IWOS'2000, Hanoi, Vietnam, 473.

[4] Nguyen Van Nha, Nguen Thi Bao Ngoc, Nguyen Van Hung, *Thin Solid Film* 334 (1998) 113.

[5] K.H. Lee, Y.K.Fang, W.J.Lee, J.J.Ho, K.H.Chen, K.S.Liao, Sens. Actuators B69 (2000) 96.

[6] E. Llobet, G.Molas, P.Molinas, J.Calderer, X.Vilanova, J.Bremers, E.Sueiras, X.Correig, *J.Electrochen*, Second edition, 147 (2000) 776.

[7] M.D. Antonik, J.E.Scheinder,E.L.Wittman,K.Snow, J.F.Vetelino, R.J.Cad, *Thin Solid Film* 256 (1995) 247.

[8] K.J. Lethy, D.Beena, R.Vinod Kumar, V.P.Mahadevan Pillai, V.Ganesan, V.Sathe, D.M.Phase, *Appli. Phys* A91 (2008) 638.

[9] S.C. Moulzolf, L.J. LeGore, R.J. Lad, *Thin solid films* 400 (2001) 56.

[10] Huiyao Wang, Pei Xu, Tianmin Wang, *Thin solid films* 388 (2001) 68.

[11] Christian Salinga, Hansjörg Weis, Matthias Wuttig, *Thin solid films* 414 (2002) 275.

[12] Toshikazu Nishide, Fujio Mizukami, *Thin solid films* 295 (1995) 212.

[13] A. Elshafie, H.H. Afify, A. Abdel-All, *phys. stat. sol.* (a) 174 (1999) 301.

[14] P.S. Patil, P.R.Patil, E.A. Ennaoui, *Thin solid films* 370 (2000) 38.

[15] M.J. Hutchins, N.A. Kamel, N. El-Kadry, A.A. Ramadan, K. Abdel-Hady, *phys. stat. sol.* (a) 175 (1999) 991.

[16] P.V. Ashrit, *Thin solid films* 385 (2001) 81.

[17] G. Macrelli, E. Poli, H. Demiryont, R.Götzelmann, *Journal of non-crystalline solids* 218 (1997) 296.

[18] G. Leltheriotis, S. Papaefthimiou, P. Yianoulis, A. Siokou, *Thin solid films* 384 (2001) 298.

[19] H.Y. Wong, C.W.Ong, R.W.M. Kwok, K.W. Wong, S.P. Wong, W.Y. Cheung, *Thin solid films* 376 (2000) 131.

[20] I. Forqueras, E. Bertran, *Thin solid films* 377-378 (2000) 8.

[21] J.H. Huh, H.R. Hwang, J.H. Paik, D.D. Lee, J.O.Lim, *Thin solid films*, 385 (2001) 255.

[22] JCPDS, JCPDS diffraction tables, *International centre for diffraction data* 1997.

[23] Le Van Ngoc, Tran Tuan, Nguyen Van Den, Duong Ai Phuong, Huynh Thanh Dat, Tran Cao Vinh, Cao Thi My Dung. *Science & technology Development VNU-HCMC*, Vol. 8, 08/2005.

[24] S.H.Lee, H.M.Cheong, C.E.Tracy, A.Mascarenhas, D.K.Benson, S.K.Deb Electrochim. Act. 44 (1999) 3111.

[25] E.Cazzanelli, L.Papalino, A.Pennisi, F.Simone, *Electrochimica Acta* 46 (2001) 1937.

[26] E. Cazzanelli, C. Vinegoni, G. Mariotto, A. Kuzmin, J. Purans, *Solid State Ionics* 123 (1999) 67.